Direct and Inverse Cascades in Turbulent Bose-Einstein Condensates

Ying Zhu,[1,*] Boris Semisalov,[2,3,4] Giorgio Krstulovic,[2] and Sergey Nazarenko[1]
[1]Université Côte d'Azur, CNRS, Institut de Physique de Nice (INPHYNI), Parc Valrose, 06108 Nice, France
[2]Université Côte d'Azur, Observatoire de la Côte d'Azur, CNRS, Laboratoire Lagrange, Boulevard de l'Observatoire CS 34229—F 06304 Nice Cedex 4, France
[3]Novosibirsk State University, 1 Pirogova street, 630090 Novosibirsk, Russia
[4]Sobolev Institute of Mathematics SB RAS, 4 Academician Koptyug Avenue, 630090 Novosibirsk, Russia

(Received 14 September 2022; revised 4 November 2022; accepted 21 February 2023; published 27 March 2023)

When a Bose-Einstein condensate (BEC) is driven out of equilibrium, density waves interact nonlinearly and trigger turbulent cascades. In a turbulent BEC, energy is transferred toward small scales by a direct cascade, whereas the number of particles displays an inverse cascade toward large scales. In this work, we study analytically and numerically the direct and inverse cascades in wave-turbulent BECs. We analytically derive the Kolmogorov-Zakharov spectra, including the log correction to the direct cascade scaling and the universal prefactor constants for both cascades. We test and corroborate our predictions using high-resolution numerical simulations of the forced-dissipated Gross-Pitaevskii model in a periodic box and the corresponding wave-kinetic equation. Theoretical predictions and data are in excellent agreement, without adjustable parameters. Moreover, in order to connect with experiments, we test and validate our theoretical predictions using the Gross-Pitaevskii model with a confining cubic trap. Our results explain previous experimental observations and suggest new settings for future studies.

DOI: 10.1103/PhysRevLett.130.133001

In many nonlinear systems, a nontrivial out-of-equilibrium state emerges when dissipation and injection of some invariant (typically energy) occur at very different scales. Such states are often characterized by a constant flux across scales of the invariant in a cascade process. In general terms, the process where an invariant is transferred from large to small scales is called a *direct cascade*, whereas the opposite is an *inverse cascade*. Such cascades play a central role in hydrodynamic and wave turbulence. In the former case, they are powered by hydrodynamic vortex interactions, whereas in the latter case they are powered by interactions of random waves. There are numerous important physical examples of wave turbulence (WT) in nature: among many others, turbulence of inertial and internal waves in rotating stratified fluids [1,2], gravitational waves [3], Kelvin waves in superfluids vortices [4], and Bose-Einstein condensates (BECs) [5]. Unlike hydrodynamic turbulence—where most predictions remain phenomenological—when waves are "weak," WT theory furnishes analytical predictions for the wave excitation spectrum which can be found as exact solutions of an associated wave kinetic equation (WKE). It expresses the spectrum in terms of the flux and wave numbers, predicts the direction of the cascades, and provides the values of the universal proportionality constants [6].

Remarkably, recent experiments with BECs have succeeded in achieving controlled WT processes in the direct energy cascade setting [7,8]. Intriguingly, those experiments measured a notably steeper (in wave number) spectrum than the one predicted by the theory [5]. In addition to being a fundamentally important state of matter, BECs have great potential as a platform for experiments in turbulence, both vortex and wave kinds. This richness is due to the close analogy between the BEC motion and the classical fluid flow. Because of the versatility of current optical techniques, BEC experiments allow a great deal of flexibility often unavailable in classical fluid experiments. Moreover, the Gross-Pitaevskii equation (GPE), which describes BEC dynamics, is a universal nonlinear model whose importance spans diverse physical systems, particularly in optics, plasmas, and water wave theory [5].

In this Letter, we study the direct and inverse cascades of turbulent BECs. We use the GPE description of a BEC and its associated WKE. We obtain new analytical predictions, which explain the steeper spectrum observed in Ref. [7], and provide the values of the dimensionless universal constants in the direct energy and inverse particle cascades. Our predictions are then tested by high-resolution direct numerical simulations of the GPE and its associated four-wave WKE.

The dimensionless GPE equation for the complex wave function $\psi(\mathbf{x}, t)$ is

$$\frac{\partial \psi(\mathbf{x}, t)}{\partial t} = i[\nabla^2 - |\psi(\mathbf{x}, t)|^2 + U(\mathbf{x})]\psi(\mathbf{x}, t), \qquad (1)$$

where $U(\mathbf{x})$ is an external trapping potential. Equation (1) is obtained from the standard dimensional GPE by a proper rescaling of time and space; see Supplemental Material

(SM) [9]. For simplicity, in the first part of this Letter, we study a homogeneous ($U = 0$) three-dimensional BEC. We consider the GPE in a triply periodic cube of side L and volume $V = L^3$. GPE (1) conserves the total number of particles and energy per unit of volume,

$$N = \frac{1}{V}\int_V |\psi(\mathbf{x},t)|^2 d\mathbf{x}, \tag{2}$$

$$H = \frac{1}{V}\int_V [|\nabla\psi(\mathbf{x},t)|^2 + \frac{1}{2}|\psi(\mathbf{x},t)|^4] d\mathbf{x}, \tag{3}$$

respectively.

When the condensate is negligible, the WT theory for the GPE formulates an asymptotic closure for the wave action spectrum $n_{\mathbf{k}}(t) \equiv n(\mathbf{k},t) = [V/(2\pi)^3]\langle|\hat{\psi}_{\mathbf{k}}(t)|^2\rangle$, where $\hat{\psi}_{\mathbf{k}}(t)$ is the Fourier transform of $\psi(\mathbf{x},t)$, and the brackets denote averaging over the initial wave statistics. The WT closure is derived under assumptions of small nonlinearity and random initial phases and amplitudes of waves [6,10]. It furnishes a wave-kinetic equation with four-wave interactions [5,11]. For an isotropic spectrum, which depends only on the magnitude of the wave vector $k = |\mathbf{k}|$, it is given by [12,13]

$$\frac{\partial n_k}{\partial t} = \mathrm{St}_k(t) \equiv \frac{32\pi^3}{k}\int_{k_i>0} \min(k,k_1,k_2,k_3) k_1 k_2 k_3 \times n_k n_{k_1} n_{k_2} n_{k_3}\left(\frac{1}{n_k}+\frac{1}{n_{k_1}}-\frac{1}{n_{k_2}}-\frac{1}{n_{k_3}}\right)\delta(\omega_{23}^{01}) dk_1 dk_2 dk_3, \tag{4}$$

where $\omega_{23}^{01} \equiv \omega_k + \omega_{k_1} - \omega_{k_2} - \omega_{k_3}$, with $\omega_k = \omega(k)$ being the frequency given by the dispersion relation $\omega_k = k^2$.

The WKE conserves the densities of the number of particles and the energy,

$$N = 4\pi\int_0^\infty k^2 n_k dk, \quad E = 4\pi\int_0^\infty k^4 n_k dk, \tag{5}$$

which coincide with Eq. (2) and with the first term of the integrand in Eq. (3) (the second term is small), respectively.

It is well known that the four-wave WKE may have two Kolmogorov-Zakharov- (KZ) type nonequilibrium stationary solutions. KZ solutions are expected in forced-dissipated wave systems in which WT is forced and dissipated at small and large wave vectors, respectively, for a direct cascade, and vice versa for an inverse cascade.

To find stationary solutions, we assume a power-law spectrum in the form $n_k = Ak^{-2x}$. The right-hand side (rhs) of Eq. (4) becomes $\mathrm{St}_k = 4\pi^3 A^3 k^{4-6x} I(x)$, where

$$I(x) = \int [\min(1,q_1,q_2,q_3)]^{1/2}(1+q_1^x - q_2^x - q_3^x) \times (q_1 q_2 q_3)^{-x}\delta(q_{23}^{01}) dq_1 dq_2 dq_3, \quad q_i > 0, \tag{6}$$

is the dimensionless collision term depending only on x, and $\delta(q_{23}^{01}) = \delta(1 + q_1 - q_2 - q_3)$. Zakharov's transformation (ZT) allows finding stationary solutions [zeros of $I(x)$] by mapping the integration subdomains into a single triangle [6] as follows:

$$\begin{aligned}
&q_2 = \frac{1}{\widetilde{q}_2}, \quad q_1 = \frac{\widetilde{q}_3}{\widetilde{q}_2}, \quad q_3 = \frac{\widetilde{q}_1}{\widetilde{q}_2}, \quad \text{for } q_2 > 1, \quad 0 < q_3 < 1,\\
&q_3 = \frac{1}{\widetilde{q}_3}, \quad q_1 = \frac{\widetilde{q}_2}{\widetilde{q}_3}, \quad q_2 = \frac{\widetilde{q}_1}{\widetilde{q}_3}, \quad \text{for } 0 < q_2 < 1, \quad q_3 > 1,\\
&q_1 = \frac{1}{\widetilde{q}_1}, \quad q_2 = \frac{\widetilde{q}_3}{\widetilde{q}_1}, \quad q_3 = \frac{\widetilde{q}_2}{\widetilde{q}_1}, \quad \text{for } q_2, q_3 > 1.
\end{aligned} \tag{7}$$

After dropping tildes, $I(x)$ becomes

$$I_{\mathrm{ZT}}(x) = \int q_1^{1/2-x}(q_2 q_3)^{-x}(1+q_1^x - q_2^x - q_3^x) \times (1+q_1^y - q_2^y - q_3^y)\delta(q_{23}^{01}) dq_1 dq_2 dq_3, \quad 0 < q_i < 1, \tag{8}$$

where $y = 3x - 7/2$. $I_{\mathrm{ZT}}(x) = 0$ has two apparent solutions, $x = 7/6$ and $x = 3/2$, corresponding to the nonequilibrium stationary inverse cascade $n_k \sim k^{-7/3}$ and direct cascade $n_k \sim k^{-3}$, respectively. One should always substitute these candidate x values into $I(x)$ to ensure that the resulting integral is convergent and equal to zero, since ZT is not an identity transformation. Such an integral convergence, called the interaction locality, physically means that wave quartets with similar values of wave numbers dominate the nonlinear evolution. Mathematically, violation of locality simply means that the considered spectrum is not a valid stationary solution of the WKE. Note that under the locality assumption $I_{\mathrm{ZT}}(x) = I(x)$.

Consider first the inverse cascade of particles. According to Eqs. (4) and (5), the spectral flux of particles through the sphere of radius $|k|$ on the spectrum $n_k = Ak^{-2x}$ is

$$Q(k) \equiv -4\pi\int_0^k \kappa^2 \mathrm{St}_\kappa d\kappa = 8\pi^4 A^3 k^{7-6x}\frac{I_{\mathrm{ZT}}(x)}{3x-7/2}. \tag{9}$$

When $x \to 7/6$, one can use the l'Hôpital rule to derive a constant (k-independent) particle flux thanks to the locality of $I(7/6)$ (see SM [9]): $Q_0 = 8\pi^4 A^3 I'_{\mathrm{ZT}}(7/6)/3$, where $I'_{\mathrm{ZT}}(x) = dI_{\mathrm{ZT}}(x)/dx$. Thus, $A = C_i|Q_0|^{1/3}$, where $C_i > 0$ is a dimensionless universal constant [recall that $Q_0 < 0$, but $I'_{\mathrm{ZT}}(7/6) < 0$ in SM [9]]. We calculate C_i analytically in SM, and write the resulting KZ spectrum for the inverse cascade as

$$n_k = C_i|Q_0|^{1/3}k^{-7/3}, \quad C_i \approx 7.5774045 \times 10^{-2}. \tag{10}$$

Now, let us consider the direct cascade. The energy flux per unit of volume is defined as $P(k) \equiv 4\pi\int_0^k \kappa^4 \mathrm{St}_\kappa(x) d\kappa$. It appears that this integral is logarithmically divergent for

$x = 3/2$, i.e. marginally nonlocal. Interestingly, we found $I(3/2)$ is finite but nonzero, which means that $n_k \sim k^{-3}$ for a constant direct energy flux obtained by dimensional analysis is not a valid mathematical solution of the WKE and is not physically realizable. Based on a phenomenological argument analogous to Kraichnan's well-known argument for the log correction of the direct enstrophy cascade spectrum in the classical 2D turbulence [14], Refs. [5,6] proposed a "log correction" for k^{-3}. Note that the universal prefactor constant cannot be determined using such an argument due to its nonrigorous nature. To address the log correction systematically, we introduce an IR cutoff at the forcing wave number k_f in the energy flux integral, then $n_k = Ak^{-3}$ leads to $P(k) = -16\pi^4 A^3 I(\frac{3}{2}) \ln(k/k_f)$ for $k > k_f$, which is not k independent as assumed by the KZ spectrum. Instead, we seek for a solution of the form $n_k = Bk^{-2x}\ln^z(k^2/k_f^2)$, then $P(k)$ can be simplified for $k \gg k_f$ as

$$P(k) = -16\pi^4 B^3 I(x) \ln^{3z}\left(\frac{k^2}{k_f^2}\right) \int_{k_f}^{k} \kappa^{8-6x} d\kappa. \quad (11)$$

Constant energy flux requires $x = 3/2$ and $z = -1/3$, giving $P_0 = -16\pi^4 B^3 I(3/2)$. Finally, we obtain the log-corrected KZ spectrum for the direct cascade and the universal prefactor as

$$n_k = C_d P_0^{1/3} k^{-3} \ln^{-1/3}(k/k_f), \qquad C_d \approx 5.26 \times 10^{-2}. \quad (12)$$

All the details for the derivation of KZ spectra can be found in the SM [9].

Note that previous GPE numerical simulations in the direct cascade setting [15,16] reported a reasonable agreement with the -3 power-law scaling of Eq. (12), but the numerical resolution was rather limited and no log correction was observed or discussed. In numerical simulations of Ref. [7], a steeper scaling with exponent close to -3.5 was reported, which was similar to the experimental result discussed in the same Letter. The scale separation there was also relatively modest, and no explanation was given for the steeper spectrum. As for the inverse cascade, to date there have been no numerical simulations or experiments done.

We perform numerical simulations of the forced-dissipated GPE using the standard massively parallel pseudo-spectral code FROST [17] with a fourth-order exponential Runge-Kutta temporal scheme (see Ref. [13]). We use grids of N_p^3 collocation points, with $N_p = 512$ and $N_p = 1024$ to verify the numerical convergence. We add a forcing term $F_{\mathbf{k}}(t)$ and a dissipation term $-D_{\mathbf{k}}\hat{\psi}_{\mathbf{k}}(t)$ to the Fourier transform of the rhs of GPE (1). The forcing term is supported on a narrow band around the forcing wave number k_f and it obeys the Ornstein-Ulenbeck process $dF_{\mathbf{k}}(t) = -\gamma\hat{\psi}_{\mathbf{k}}dt + f_0 dW_{\mathbf{k}}$, where $W_{\mathbf{k}}$ is the Wiener process. The parameters γ and f_0 control the correlation time and the amplitude of the forcing, respectively. Naturally, k_f is taken small for the direct cascade and large for the inverse one. Dissipation is of the form $D_{\mathbf{k}} = (k/k_L)^{-\alpha} + (k/k_R)^{\beta}$, and acts at small and large scales. Moreover, the condensate ($k = 0$ mode) is dissipated in the same manner with a constant friction $D_{\mathbf{0}}$. We optimize the parameters of forcing and dissipation in order to enlarge the inertial range for a fixed resolution, while maintaining simulations well resolved and minimizing bottlenecks at the dissipation scales. We pay special attention that forcing is weak enough so that the system fulfills WT assumptions (see SM for verification [9]). Table I gives numerical parameters. Finally, the k-space energy and particle fluxes, $P(k)$ and $Q(k)$, respectively, are computed directly using the GPE (1) (see SM and Ref. [18]).

We also simulate the WKE with forcing and dissipation using the code developed in Refs. [13,19]. This code solves the WKE expressed in wave frequency ω, and uses a decomposition of the integration domain of the rhs of Eq. (4) along lines where the integrand has discontinuous derivatives. The WKE is solved in the interval $\omega \in [\omega_{\min}, \omega_{\max}]$, and we set $n_\omega = n_{\omega_{\min}}$ for $\omega < \omega_{\min}$ and $n_\omega = 0$ for $\omega > \omega_{\max}$. The WKE is forced by a constant-in-time forcing $f_\omega = c_f G(\omega)$, where $G(\omega)$ is a Gaussian centered at ω_f and of width $\Delta\omega_f$. Dissipation is introduced by adding the term $-[(\omega/\omega_L)^{-\alpha} + (\omega/\omega_R)^{\beta}]n_\omega$ to the rhs of WKE. For time integration, we use a new approach inspired by Chebyshev interpolation and schemes described in Ref. [20]. Values of the parameters are reported in Table I. In this Letter, we present solutions of the WKE in k variables to simplify comparisons with GPE data. Standard WKE-based k-dependent fluxes are given in the SM [9].

TABLE I. Parameters for GPE and WKE simulations.

Case	Model	Cascade	L	N_p	f_0^2	γ
1	GPE	direct	2π	512	1.2	20
2			4π	1024	0.1589	
3		inverse	2π	512	10^{-4}	0
4			4π	1024	1.26×10^{-5}	
Case	k_f	$D_{\mathbf{0}}$	k_L	α	k_R	β
1, 2	8	10^3	2.5	2	145	4
3, 4	125		1	0.5	130	6
Case	Model	Cascade	$\omega_{\min}$	$\omega_{\max}$	ω_f	c_f
5	WKE	direct	10^{-5}	10	3×10^{-4}	1
6		inverse	0.1	10^5	125^2	50
Case	$\Delta\omega_f$	ω_L	α	ω_R	β	k_f
5	3×10^{-4}	10^{-4}	3	2	4	$\sqrt{10^{-3}}$
6	500	10	4	$10^5/4.5$	7	125

First, we present numerical results for the direct cascade state. Figure 1 displays the stationary wave action spectra obtained in simulations of the GPE and the WKE, respectively, both compensated by the theoretical prediction Eq. (12). The inset shows their respective scale-dependent energy fluxes, normalized by P_0 measured in the range where $P(k)$ is approximately constant. The same values of P_0 are used in Eq. (12). The values of k_f, as presented in Table I, are selected within the range of forcing. For comparison, we also plot the compensated KZ spectra $\sim n_k k^3$ (ignoring the nonlocality issue) and $\sim n_k k^{3.5}$ for the GPE data with $N_p = 1024$. We see an excellent agreement between Eq. (12) and GPE and WKE data including the value of the constant C_d. The vertical dotted line denotes the wave vector k_ξ where the nonlinear term in the GPE becomes equal to the linear one. WT prediction is expected to be valid at $k > k_\xi$ only. Further, the asymptotic result Eq. (12) is assumed for $k \gg k_f$. Interestingly, the theoretical log-corrected KZ spectrum provides a very good fit to the numerical results even at the scales $k \lesssim k_\xi \sim k_f$. Note that GPE data with $N_p = 1024$ present a relatively good agreement with $k^{-3.5}$ too, although in a much narrower range and only at low k, which is consistent with the results reported in Ref. [7].

Next, we study the inverse cascade state. Figure 2 shows the wave action spectra and the particle fluxes $Q(k)$ (in inset normalized by $|Q_0|$) obtained in GPE and WKE simulations. Spectra are compensated by the theoretical prediction Eq. (10) including the value of the prefactor C_i. Again, for GPE data we mark k_ξ by a vertical dotted line. For both GPE and WKE we see a significant range (within the constant-Q region) where the compensated spectra have plateaus, which confirms the predicted spectrum Eq. (10). The agreement between theory and numerics is almost perfect for WKE data and within 5% for GPE. Note that in both simulations we see a "bump" on the left-hand part of the spectrum, which could be attributed to an infrared bottleneck caused by the nature of the hypoviscous dissipation.

Finally, to check the reliability of our predictions in a setting closer to experiments, we study the direct and inverse cascades for BEC trapped in a cubic box. To this end, while solving Eq. (1) we consider a trapping potential $U(\mathbf{x})$ that vanishes inside the box and increases rapidly at the borders of the cube (see SM for an exact definition [9]). Figure 3(a) displays a two-dimensional cut of a typical simulation where we plot the trapping potential and the wave field. We keep the same forcing and dissipation schemes and the parameters of case 1 and case 3 in Table I, respectively. The results for both the direct and the inverse cascades are shown in Fig. 3, superimposed with the theoretical KZ spectra (solid lines) without any fitting parameters. Once again, one can see a nearly perfect agreement, which indicates robustness of our theoretical predictions and their relevance to the past and future experiments on BEC turbulence. It might be convenient for comparison with experiments to rewrite our predictions [Eqs. (12) and (10)] in dimensional form. In terms of the reduced Planck constant $\hbar$, the interaction constant g and boson mass m, they read (see SM [9])

$$\text{direct}: n_k = C_d (P_0 \hbar/g^2)^{1/3} k^{-3} \ln^{-1/3}(k/k_f), \tag{13}$$

$$\text{inverse}: n_k = C_i (|Q_0|\hbar^3/2g^2 m)^{1/3} k^{-7/3}. \tag{14}$$

Note the n_k is dimensionless and normalized such that $N = \int n_k d^3\mathbf{k}$ is the total number of particles per unit of volume.

Summarizing, in this Letter we have derived the stationary direct and inverse cascade KZ spectra [Eqs. (10) and (12)], including, for the first time, the analytical determination of the logarithmic correction in Eq. (12) and the prefactor constants for both. Our predictions are in

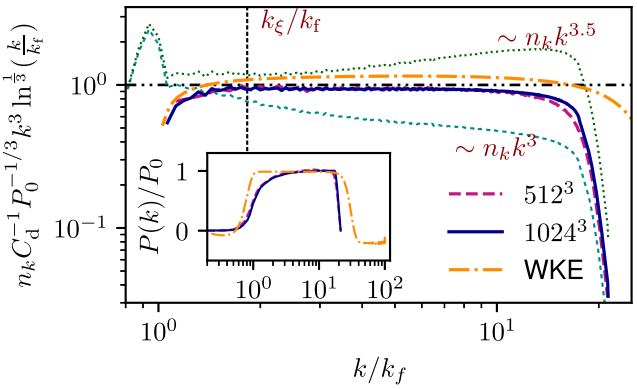

FIG. 1. Wave action spectra for the direct cascade compensated by theoretical prediction [Eq. (12)]. Data obtained by GPE at two different resolutions and by WKE, respectively. Inset: corresponding energy fluxes normalized by their values measured in inertial range.

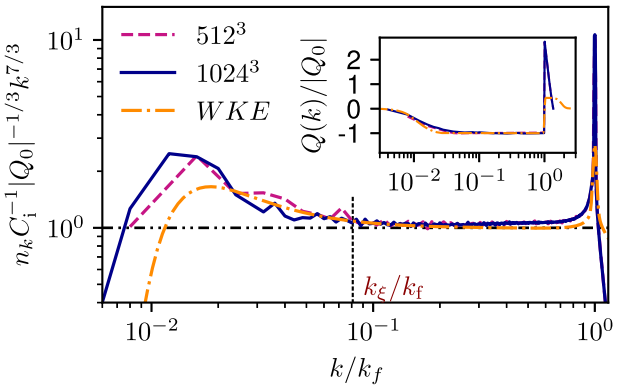

FIG. 2. Wave action spectra for the inverse cascade compensated by theoretical prediction [Eq. (10)]. Data obtained by GPE at two different resolutions and by WKE, respectively. Inset: corresponding particle fluxes normalized by their values measured in inertial range.

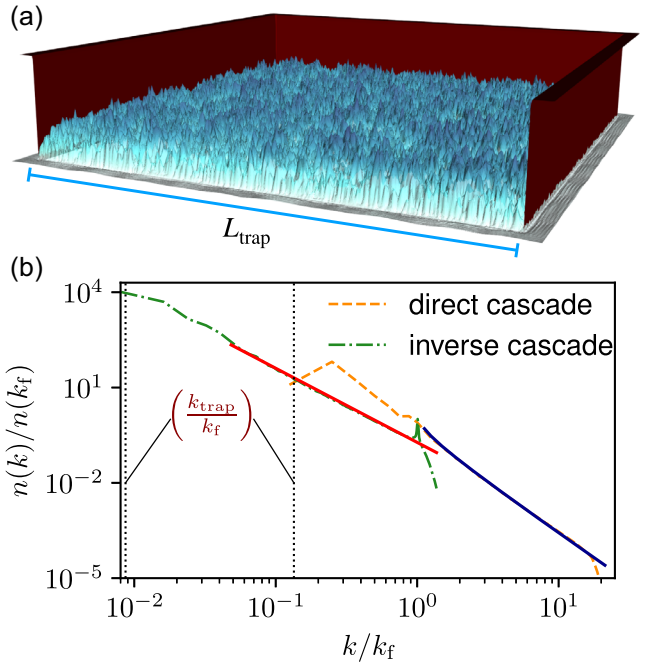

FIG. 3. GPE simulations of turbulent trapped BEC. (a) Two-dimensional cut of a typical simulation (arbitrary units and scales). The trapping potential is displayed in red and density fluctuations in blue. (b) Wave action spectra normalized by their values at the respective forcing scales k_f for the direct and the inverse cascades. The solid lines display the theoretical predictions [Eqs. (10) and (12)]. The vertical lines show the wave number $k_{\text{trap}} = 2\pi/L_{\text{trap}}$ for both of the cascades, with L_{trap} the trap size.

remarkable agreement, without any adjustable parameters, with numerical simulations of the GPE and the WKE. Such definitive agreement was possible thanks to considerable higher than in the previous works resolution of the GPE simulations and careful checks of the WT assumptions. To our knowledge, we also presented the first simulations of the associated WKE in the steady state regimes.

In the case of the direct cascade, previous works reported a steeper -3.5 exponent [7]—a result which deviates from the dimensional WT prediction -3. Several processes (a residual role of vortices, the non-negligible incompressible-flow energy, an increasing importance of quantum pressure) were suggested in Ref. [7] as candidates for explaining the experimental result but without an argument of why they could lead to the $k^{-3.5}$ spectrum. We do not think that such additional processes are important and/or need to be considered because the logarithmic correction in Eq. (12) was derived without invoking other physical phenomena than weak wave turbulence. It is convincingly confirmed by our high-resolution numerical results and it agrees with the experimental spectrum reported in Ref. [7] (see SM [9]). Hence, we conclude that the spectrum $k^{-3.5}$ is an approximation to the log-corrected KZ spectrum. Further, for the first time, in our work the inverse cascade KZ spectrum is observed numerically.

Our results are useful for laboratory experiments, and we have validated them with simulations of GPE of a trapped BEC. In the future, it would be particularly interesting to have a stationary inverse cascade state experimentally implemented. For this, one could use a similar forcing technique as in Refs. [7,8], namely shaking the retaining trap. In addition, one would have to devise a synthetic dissipation mechanism removing low momentum atoms which would prevent their accumulation (condensation) near the ground state of the trap, thereby making a statistically steady state possible.

This work was funded by the Simons Foundation Collaboration grant Wave Turbulence (Award No. 651471). This work was granted access to the high-performance computing facilities under GENCI (Grand Equipement National de Calcul Intensif) A0102A12494 (IDRIS and CINES), the OPAL infrastructure from Université Côte d'Azur, supported by the French government, through the UCAJEDI Investments in the Future project managed by the National Research Agency (ANR) under Reference No. ANR-15-IDEX-01, and the SIGAMM infrastructure hosted by Observatoire de la Côte d'Azur, supported by the Provence-Alpes Côte d'Azur region and supported by the state contract of the Sobolev Institute of Mathematics (Project No. FWNF-2022-0008).

*yzhu@unice.fr

[1] P. Caillol and V. Zeitlin, Dyn. Atmos. Oceans **32**, 81 (2000).
[2] S. Galtier, Phys. Rev. E **68**, 015301(R) (2003).
[3] S. Galtier and S. V. Nazarenko, Phys. Rev. Lett. **119**, 221101 (2017).
[4] V. S. L'vov and S. Nazarenko, Low Temp. Phys. **36**, 785 (2010).
[5] S. Dyachenko, A. Newell, A. Pushkarev, and V. Zakharov, Physica (Amsterdam) **57D**, 96 (1992).
[6] S. Nazarenko, *Wave Turbulence* (Springer Science & Business Media, Heidelberg, 2011), Vol. 825.
[7] N. Navon, A. L. Gaunt, R. P. Smith, and Z. Hadzibabic, Nature (London) **539**, 72 (2016).
[8] N. Navon, C. Eigen, J. Zhang, R. Lopes, A. L. Gaunt, K. Fujimoto, M. Tsubota, R. P. Smith, and Z. Hadzibabic, Science **366**, 382 (2019).
[9] See Supplemental Material at http://link.aps.org/supplemental/10.1103/PhysRevLett.130.133001 for extra details on theoretical calculations and numerical details.
[10] V. E. Zakharov, V. S. L'vov, and G. Falkovich, *Kolmogorov Spectra of Turbulence I* (Springer Berlin, Heidelberg, 1992), 10.1007/978-3-642-50052-7.
[11] V. Zakharov, S. Musher, and A. Rubenchik, Phys. Rep. **129**, 285 (1985).
[12] D. V. Semikoz and I. I. Tkachev, Phys. Rev. Lett. **74**, 3093 (1995).
[13] Y. Zhu, B. Semisalov, G. Krstulovic, and S. Nazarenko, Phys. Rev. E **106**, 014205 (2022).
[14] R. H. Kraichnan, Phys. Fluids **10**, 1417 (1967).

[15] D. Proment, S. Nazarenko, and M. Onorato, Phys. Rev. A **80**, 051603(R) (2009).
[16] D. Proment, S. Nazarenko, and M. Onorato, Physica (Amsterdam) **241D**, 304 (2012).
[17] G. Krstulovic, *A theoretical description of vortex dynamics in superfluids. Kelvin waves, reconnections and particle-vortex interaction*, Habilitation à diriger des recherches, (Universite Côte d'Azur, 2020), https://hal.science/tel-03544830v1.
[18] A. Griffin, G. Krstulovic, V. S. L'vov, and S. Nazarenko, Phys. Rev. Lett. **128**, 224501 (2022).
[19] B. Semisalov, V. Grebenev, S. Medvedev, and S. Nazarenko, Commun. Nonlinear Sci. Numer. Simul. **102**, 105903 (2021).
[20] B. V. Semisalov, Numer. Anal. Appl. **15**, 63 (2022).